CODEN IEJMAT *Internet Electronic Journal of Molecular Design* **2005**, *4*, 82–93 ISSN 1538–6414
BioChem Press http://www.biochempress.com

Inter*net* Electronic Journal of
Molecular Design

January 2005, Volume 4, Number 1, Pages 82–93

Editor: Ovidiu Ivanciuc

On the Mechanism of Glycoside Hydrolysis by the Family GH–90 Phage P22 Tailspike Protein

Wim Nerinckx,[1] Tom Desmet,[1] and Marc Claeyssens [1]

[1] Laboratory for Glycobiology, Department of Biochemistry, Fysiology and Microbiology, Ghent University, K. L. Ledeganckstraat 35, B–9000 Ghent, Belgium

Received: September 6, 2004; Accepted: November 14, 2004; Published: January 31, 2005

Citation of the article:
W. Nerinckx, T. Desmet, and M. Claeyssens, On the Mechanism of Glycoside Hydrolysis by the Family GH–90 Phage P22 Tailspike Protein, *Internet Electron. J. Mol. Des.* **2005**, *4*, 82–93, http://www.biochempress.com.

Internet Electronic Journal of Molecular Design

BioChem Press
http://www.biochempress.com

On the Mechanism of Glycoside Hydrolysis by the Family GH–90 Phage P22 Tailspike Protein

Wim Nerinckx,[1,*] Tom Desmet,[1] and Marc Claeyssens [1]

[1] Laboratory for Glycobiology, Department of Biochemistry, Fysiology and Microbiology, Ghent University, K. L. Ledeganckstraat 35, B–9000 Ghent, Belgium

Received: September 6, 2004; Accepted: November 14, 2004; Published: January 31, 2005

Internet Electron. J. Mol. Des. **2005**, *4* (1), 82–93

Abstract

The mechanism of the glycoside hydrolase family 90 *Salmonella* phage P22 tailspike protein was reevaluated by automated docking using Autodock3, with O–antigen oligosaccharide fragments having different ring–conformations at L–rhamnose and that span the essential –1 to +1 subsites. In contrast to a previously suggested mechanism, the docking results strongly indicate that an ALPH–compliant inverting mechanism is operative, with an anti–positioned Asp395 acting as proton donor and with Asp392 as general base assistant.

Keywords. Glycoside hydrolase; AutoDock; docking; active site; ALPH; antiperiplanar lone pair hypothesis.

Abbreviations and notations

Abe, abequose (D–3,6–dideoxygalactopyranose)	ALPH, Antiperiplanar Lone Pair Hypothesis
ADT, AutoDockTools	LGA, Lamarckian Genetic Algorithm

1 INTRODUCTION

The *Salmonella* phage P22 capsid contains at the base of its neck structure up to six identical tailspike protein molecules. They are non–covalently bound and function as a viral adhesion factor to the bacterial host. The cellular receptor is the O–antigenic multiple–repeating trisaccharide [→2)–α–D–mannopyranosyl–(1→4)–α–L–rhamnopyranosyl–(1→3)–α–D–galactopyranosyl–(1→] of a *Salmonella* lipopolysaccharide [1,2]. The host range includes serotypes A, B and D1 which are characterised by a non–pervasive occurrence of 3,6–dideoxyhexoses, respectively paratose, abequose and tyvelose, α–(1→3)–linked to D–mannose of the linear O–antigen polysaccharide. It also accepts the O–antigen 12_2 variant of serotype D1, which is characterised by the extra presence of single α–(1→4)–D–glucosyl units at the main chain's D–galactose [3–6]. The tailspike protein consists of a small (12 kDa) N–terminal, dome–like, head binding domain, and a large (60 kDa) elongated C–terminal fish–shaped domain which carries the O–antigen binding and cleavage site

* Correspondence author; E–mail: wim.nerinckx@ugent.be.

[7.8]. The active site (a long central cleft) lines the main axis of the 150 Å long protein, and is large enough to accommodate three antigenic repeats; two repeats are sufficient for receptor binding. It slowly cleaves the α–(1→3) *O*–glycosidic bond between L–rhamnose and D–galactose [9], and has been classified as a Glycoside Hydrolase Family 90 endorhamnosidase [10].

The crystal structure of the active site containing C–terminal part has been determined at different resolutions. Three structures in complex with O–antigen fragments of two repeating units from serotype B, D1 and 12_2 have also been studied (PDB entries 1tyx, 1tyu, and 1tyw, respectively) [11–13]. These complexes show the oligosaccharides to reside exclusively in the enzyme's minus subsites with a terminal α–L–rhamnose occupying the –1 subsite. In all three cases, the electron density of the terminal L–rhamnose –showing a discontinuity between C2 and C3– was suggested to correspond to a $^{5}S_{1}$ skew–boat ring conformation, with the C1 hydroxyl group in α–configuration and positioned equatorially. This is remarkable, since one would expect to find the lower energy ground state (in this case a $^{1}C_{4}$) conformation in an enzyme–product complex which does not span the essential –1 to +1 subsites. Subsite –1 contains three acidic residues, Glu359, Asp392 and Asp395, and the corresponding amide mutants were shown to be enzymatically inactive without significantly reducing the substrate binding affinities [9]. Based on the relative positioning of these carboxylates versus the terminal L–rhamnose, it was proposed that Asp392 is the proton donor with Glu359 and/or Asp395 acting as general bases in an inverting mechanism [13].

The presence of a lone pair from the endocyclic oxygen that is antiperiplanar to the leaving group is a stereoelectronic requirement for heterolytic acetal C–O bond cleavage [14–17]. However, the proposed $^{5}S_{1}$ skew–boat in the tailspike protein complexes has a C1–equatorial hydroxyl group with both the endocyclic oxygen's lone pairs in synclinal position to the scissile bond. This proposed sugar conformation is contradictory to the antiperiplanar lone pair hypothesis (ALPH). For several decades, the relevance of ALPH for a glycoside hydrolysis mechanism has been the subject of debate, but has been generally accepted following a highly authoritative article by Deslongchamps [18]. As a consequence of ALPH, the hydrolysis of a β–glycoside should first undergo a conformational change away from the ground state chair to a twist–boat conformation in which the leaving group has an axial position as well as an essential set–up with an antiperiplanar ring–oxygen lone pair. In several crystal structures of β–glycoside hydrolases in complex with substrate analogues, a skew–boat conformation of the glycoside at subsite –1 has indeed been observed [19]. For α–glycosides such as the tailspike protein's O–antigen substrate, the ALPH–requirements are already met at the ground state chair conformation, suggesting their hydrolysis mechanism to proceed directly from the ground state [18].

One has to conclude that the proposed $^{5}S_{1}$ skew–boat terminal α–L–rhamnose ring conformation represents a non–productive binding mode, which prompted us to investigate other possibilities.

Indeed, in a productive Michaelis complex, with subsites –1/+1 occupied and containing an intact α–(1→3) glycosidic bond to D–Gal*p* of the next O–antigen repeat, the positioning of the L–rhamnose in subsite –1 relative to the catalytically participating amino acids could be quite different.

We presently report the use of AutoDock [20] in an effort to resolve the ambiguities of the previously proposed mechanism of glycoside hydrolysis by the family GH–90 phage P–22 tailspike protein. Dockings into a grid box containing the enzyme's –3 to +1 subsites are described, with the tetrasaccharide α–D–galactopyranosyl–(1→2)–[α–D–3,6–dideoxygalactopyranosyl–(1→3)]–α–D–mannopyranosyl–(1→4)–α–L–rhamnopyranose (rhamnose ring conformation $^5S_1$: **1**; $^1C_4$: **2**) for validation of the method, and with the crucial –1 to +1 subsites spanning pentasaccharide α–D–galactopyranosyl–(1→2)–[α–D–3,6–dideoxygalactopyranosyl–(1→3)]–α–D–mannopyranosyl–(1→4)–α–L–rhamnopyranosyl–(1→3)–α–D–galactopyranose (rhamnose ring conformation $^5S_1$: **3**; $^1C_4$: **4**; $^1S_3$: **5**) (Figure 1).

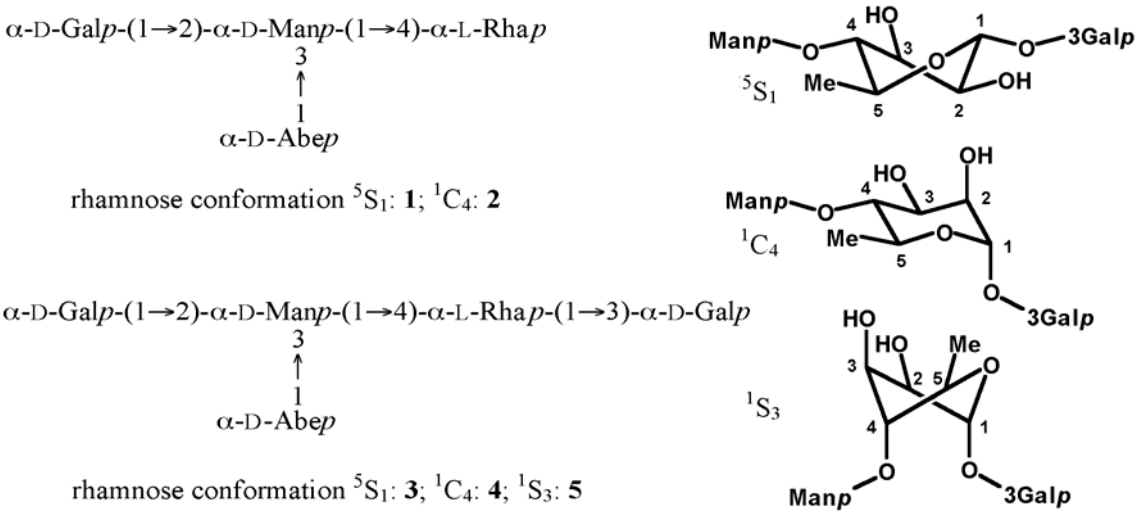

Figure 1. The tetrasaccharide and pentasaccharide used in the docking experiments: α–D–galactopyranosyl–(1→2)–[α–D–3,6–dideoxygalactopyranosyl–(1→3)]–α–D–mannopyranosyl–(1→4)–α–L–rhamnopyranose (rhamnose conformation $^5S_1$: **1**; $^1C_4$: **2**); α–D–galactopyranosyl–(1→2)–[α–D–3,6–dideoxygalactopyranosyl–(1→3)]–α–D–mannopyranosyl–(1→4)–α–L–rhamnopyranosyl–(1→3)–α–D–galactopyranose (rhamnose conformation $^5S_1$: **3**; $^1C_4$: **4**; $^1S_3$: **5**).

2 MATERIALS AND METHODS

Docking of the oligosaccharide ligands into the active site of the protein was carried out with AutoDock version 3.0.5 which includes a robust Lamarckian Genetic Algorithm (LGA) and a calibrated empirical free energy function for evaluating the conformational space of the ligand [20–22]. An excellent AutoDock–helping graphical user interface, AutoDockTools (ADT), has been released as an extension suite to the Python Molecular Viewer [23]; this allows easy and correct

formatting of the ligand and the macromolecule, as well as setting the grid and docking parameter files.

A limitation of the current AutoDock release is that it assumes the protein receptor to be rigid. In the case of phage P22 tailspike protein structures, the atoms near the crucial subsites show low B–values, and a magic fit 3D–overlay [24] with all the available 3D coordinate sets shows only very small conformational differences. Thus, the presence of a rigid receptor can in this case be regarded as a reasonable approximation.

The dockings were performed on the 3D structure from PDB entry 1tyx which contains two repeating units of the serotype B O–antigen, occupying subsites –6 to –1 [12]. Due to the absence of interpretable electron density, all available 3D structures of the P22 tailspike protein lack atomic coordinates for two short sequences: DMNPEL at 401–406 and STDGQ at 508–512. The latter segment is far away from the active site. The former segment starts after Thr400 which points the methyl group of its sidechain into the active site. This short segment then connects to Asp407 which is far away from the active site; the missing residues therefore are not essential for the integrity of the active site.

The oligosaccharide ligands were drawn and minimized with HyperChem 4.5 (MM+ force field; HyperCube Inc, Gainesville, USA) [25,26]. The ligand PDB files were subsequently converted with ADT to Gasteiger–Marsili partial charges added [27] and torsion–formatted out.pdbq files. The protein was also set–up with ADT: the ligand and all waters were removed, only polar hydrogens were added, the Kollman united–atom partial charges [28] were calculated, and atomic solvation and fragmental volumes [29] were assigned, yielding the required pdbqs file.

AutoDock uses a grid–based method for energy evaluations, in which the grid points contain precalculated affinities for the different atom types of the ligand. The number of grid points were set at 54–58–44 with a point spacing of 0.383 Å centered at 78.117–57.641–98.186, yielding a grid box that spans the –3 to +1 subsites in excess.

In the docking experiments, minor variations of the ADT 1.1 standard LGA docking parameter settings were used. The LGA–runs were started with an initial random (rotatable bond conformations, orientations and translations) population of 50 ligands that uniformly covers the grid space. The number of different docking runs were set at 50 with a run–termination of 3000 generations at a maximum of 25×10^6 energy evaluations. The elitism number, the mutation rate and the gene crossover rate were 1, 0.02 and 0.8 respectively. AutoDock uses a pseudo–Solis and Wets local search to minimize the energy of the population [30,31]. The local search frequency was 0.06 with a maximum of 300 iterations per search. The maximum consecutive successes or failures before doubling or halving the local search step size were both set to 4, with a termination criterion of 0.01. After the docking runs, the resulting oligosaccharide conformations were clustered to similarity within 3Å rms deviation.

HyperChem 4.5 ran on an SGI Indigo–II. AutoDockTools, autogrid3 and autodock3 were run on an Apple single 1600 MHz G5 or an Apple dual 450 MHz G4. Stereodrawings (wall–eyed) were prepared with the Swiss–PDB viewer 3.7 [24] and colored figures with Pymol–OSX 0.93 [32].

3 RESULTS AND DISCUSSION

3.1 Dockings with α–D–Galp–(1→2)–[α–D–Abep–(1→3)]–α–D–Manp–(1→4)–α–L–Rhap (Rhamnose Ring Conformation $^5S_1$: 1; $^1C_4$: 2)

The tetrasaccharide **1**, which has the terminal L–rhamnose in the same $^5S_1$ ring conformation as proposed in the 1tyx, 1tyu and 1tyw complex structures, was run as a test of AutoDock's predictive capability in these docking experiments. This resulted in a cluster of 48/50 alike individual conformations, of which the best–docked ($\Delta G_{binding}$; estimated free energy of binding: –6.77 kcal/mol) is shown in Figure 2. All the carbohydrate rings are in virtually the same position relative to the enzyme as in the crystal complexes, indicating that the integrity of the active site is preserved although all water molecules were removed, and, more importantly, validating the settings of the docking method. A notable feature of this (crystal as well as docked) situation is that the terminal L–rhamnose's 5–methyl group is oriented inwards to the enzyme, apparently in hydrophobic contact with the aromatic ring of Trp391.

Figure 2. Best–docked conformation of 48/50 cluster with tetrasaccharide **1** (rhamnose in $^5S_1$).

Dockings with tetrasaccharide **2**, which has a terminal L–rhamnose in the ground state $^1C_4$ ring conformation, yielded a 50/50 cluster of alike individual conformations. The best–docked ($\Delta G_{binding}$: –7.47 kcal/mol) is shown in Figure 3. The carbohydrate rings are again positioned as in the crystal complexes, with the hydrophobic 5–methyl group of the terminal L–rhamnose also in the vicinity of Trp391.

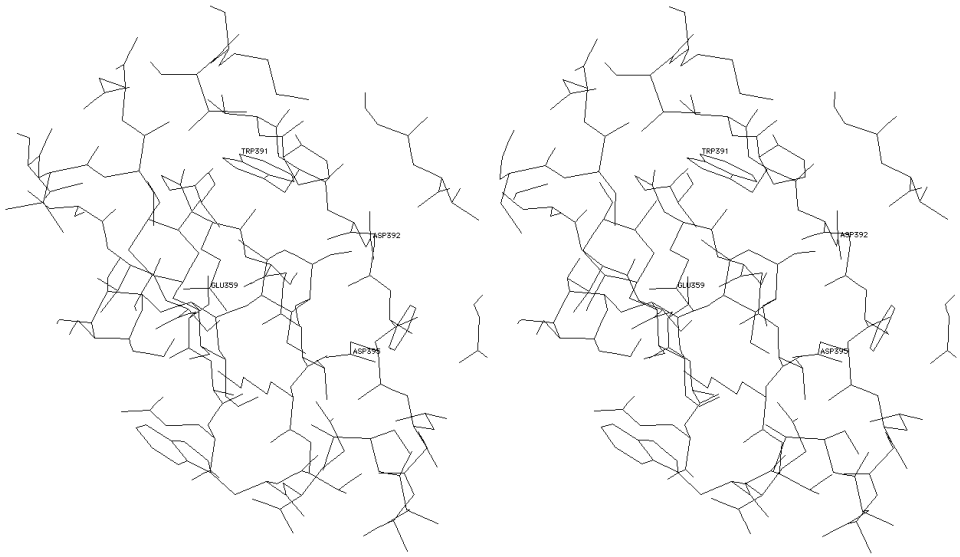

Figure 3. Best–docked conformation of 50/50 cluster with tetrasaccharide **2** (rhamnose in $^1C_4$).

Both docking results confirm the crystal complexes concerning the orientation of the terminal L–rhamnose in the –1 subsite (5–methyl group close to Trp391). However, in terms of estimated binding and docking energies, AutoDock calculates a better recognition when the L–rhamnose resides in a ground state $^1C_4$ chair. Moreover, AutoDock3 treats ring conformations as fixed and its energy minimization does not take into account the energy penalty due to the angle and torsional strains in a local minimum $^5S_1$ versus a ground state $^1C_4$ rhamnose ring. In other words, AutoDock predicts that only the latter (as in Figure 3) should be observed in these enzyme–ligand complexes.

An overlay of the coordinates of the epitope–ligand from the 1tyx crystal, including the water molecule 219 which was previously assumed to be the nucleophile [13], together with the best–docked tetrasaccharide **2**, can provide an explanation to this discrepancy (Figure 4).

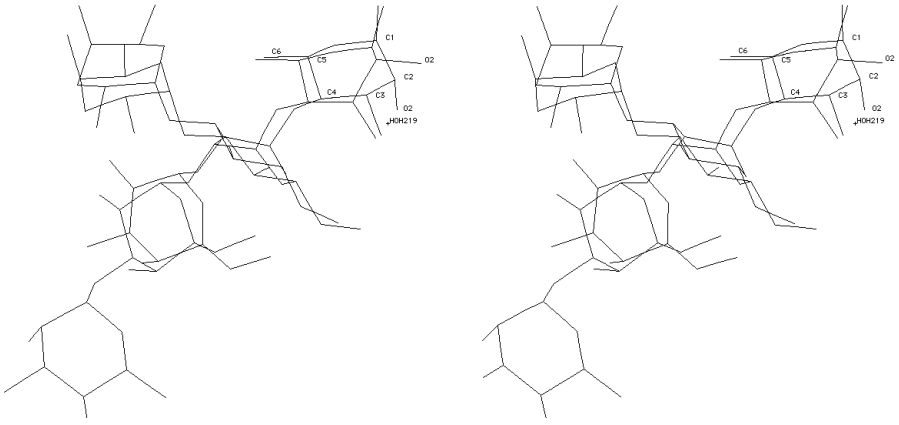

Figure 4. Overlay of the best–docked tetrasaccharide **2** (rhamnose in $^1C_4$, carbons indicated, no hydrogens shown) with the 1tyx crystal epitope fragment including the oxygen from water 219.

It is striking that the hydroxyl oxygens at C1 and C3 as well as the C5 methylgroups from both terminal rhamnoses almost coincide, whereas the C2–hydroxyl oxygen of the $^1C_4$ rhamnose has

about the same position as the oxygen of water molecule 219 in the crystal structure. It is thus very well possible that the electron density of the latter belongs to the C2–hydroxyl group of a terminal $^{1}C_{4}$ rhamnose, while the density that was attributed to a C2–hydroxyl group of a $^{5}S_{1}$ rhamnose actually originates from the oxygen of a water molecule. In the uncomplexed crystal structures, a water molecule is indeed always present at approximately this position.

3.2 Dockings with α–D–Galp–(1→2)–[α–D–Abep–(1→3)]–α–D–Manp–(1→4)–α–L–Rhap–(1→3)–α–D–Galp (Rhamnose Ring Conformation $^{5}S_{1}$: 3; $^{1}C_{4}$: 4; $^{1}S_{3}$: 5)

The added reducing–end D–galactose introduces six extra rotatable bonds to the ligand. Dockings with these pentasaccharides approach the limit of AutoDock's capability and often yielded many unrealistic binding modes at relatively high intermolecular energies. Still, each docking experiment also resulted in one or two low–energy clusters of highly alike conformations in which the non–reducing end D–Gal*p*, D–Abe*p* and D–Man*p* rings are residing in their correct subsites; these are discussed further.

Pentasaccharide **3** gave a major low–energy cluster of 20/50 similar conformations. The best–docked member ($\Delta G_{binding}$: –6.50 kcal/mol) is shown in Figure 5. The $^{5}S_{1}$ L–rhamnose within subsite –1 is turned upside down in comparison to its positioning in the crystal ligand complex, with its C2–hydroxylgroup (and not the C5–methylgroup) now pointing towards Trp391.

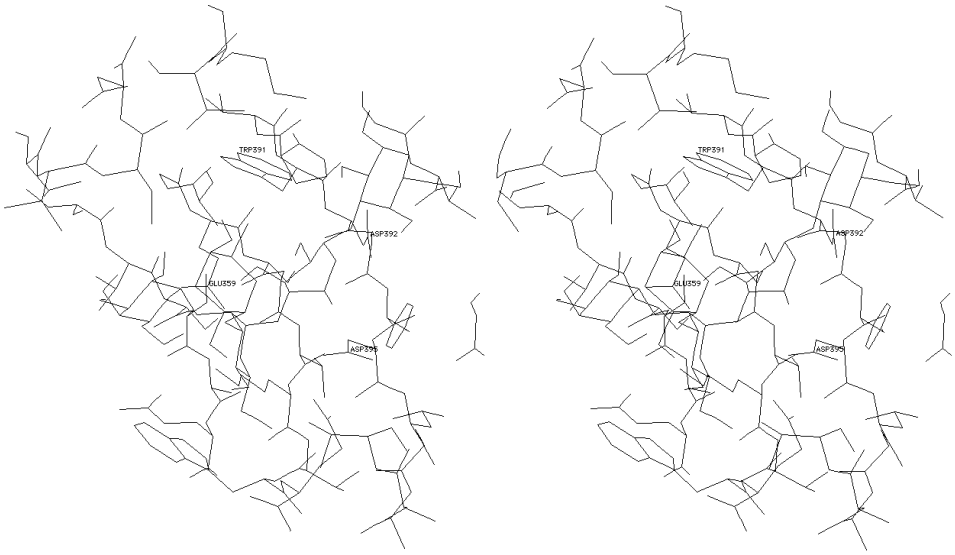

Figure 5. Best–docked conformation of 20/50 cluster with pentasaccharide **3** (rhamnose in $^{5}S_{1}$).

Apparently, a rhamnose orientation as in Figure 2 or 3 (and as observed in the crystal structure) is disfavored when a reducing end D–Gal*p* is attached. Asp392 may be close enough to the oxygen of the scissile glycosidic bond to function as proton donor, however, none of the enzyme's carboxylates is correctly positioned to be able to act as either a nucleophile or a general base.

Together with the non–ALPH compliancy of a $^{5}S_{1}$ α–L–rhamnose, the conformations in this cluster can therefore not be catalytically productive.

The dockings with pentasaccharide **4** gave two major clusters which show the non–reducing end D–Gal*p*, D–Abe*p* and D–Man*p* rings in their correct subsites. The best–docked conformation of the lowest energy cluster (7/50 similar conformations; $\Delta G_{binding}$: –9.56 kcal/mol) is shown in Figures 6, 7 and 8. The $^{1}C_{4}$ L–rhamnose at subsite –1 is again practically turned upside down in comparison to the terminal L–rhamnose from the crystal structure (the C5–methylgroup is not pointing towards Trp391). Nevertheless, this ALPH–compliant conformation shows a correct positioning of two catalytic carboxylate residues. Indeed, Asp395 is perfectly positioned, at 2.6 Å distance, to protonate the glycosidic oxygen of the axial scissile bond. Its position versus the endocyclic oxygen of L–rhamnose (close to C2, not to O5) would categorize the Family GH–90 tailspike protein as an anti–protonator [33]. Asp392 is also anti positioned but is too far away from the glycosidic oxygen to be able to act as proton donor. Although this residue is close to the anomeric center (at 3.6 Å distance), it is perpendicular to the scissile bond and is therefore unsuited for an in–line nucleophilic attack. This suggests a single–displacement (inverting) mechanism in which an in–line water molecule is the nucleophile with Asp392 being the general base assistant. In this scenario, Glu359 plays no direct mechanistic role, but appears to be important for hydrogen bonding towards the C3 hydroxyl group of the L–rhamnose at subsite –1 (at 3.0 Å distance), as well as for interactions at subsite –3. The reducing end D–Gal*p* dips deep into the active site, in a surface depression just wide enough to contain only one carbohydrate unit; this is very likely the +1 subsite (Figure 8). The axial C1 hydroxyl group of this α–D–Gal*p* points upwards and allows connection to a D–Man*p* of the next antigenic repeat.

Figure 6. Best–docked conformation of the lowest–energy 7/50 cluster with pentasaccharide **4** (rhamnose in $^{1}C_{4}$).

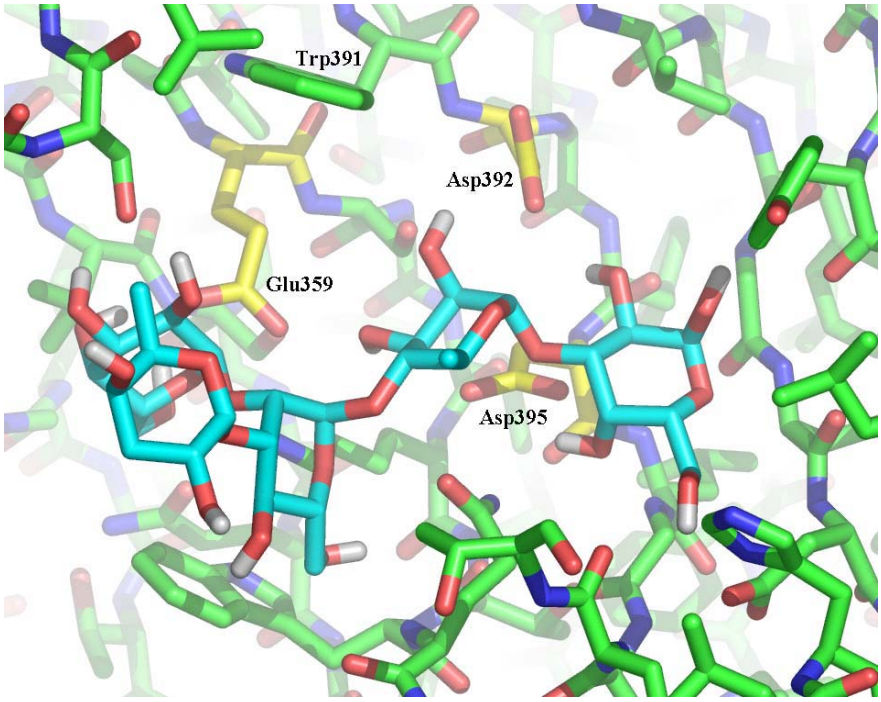

Figure 7. The situation of the best–docked pentasaccharide **4** (rhamnose in $^{1}C_{4}$, see Figure 6) in the –3/+1 subsites of the tailspike P22 protein. Carboxylate residues are coloured yellow.

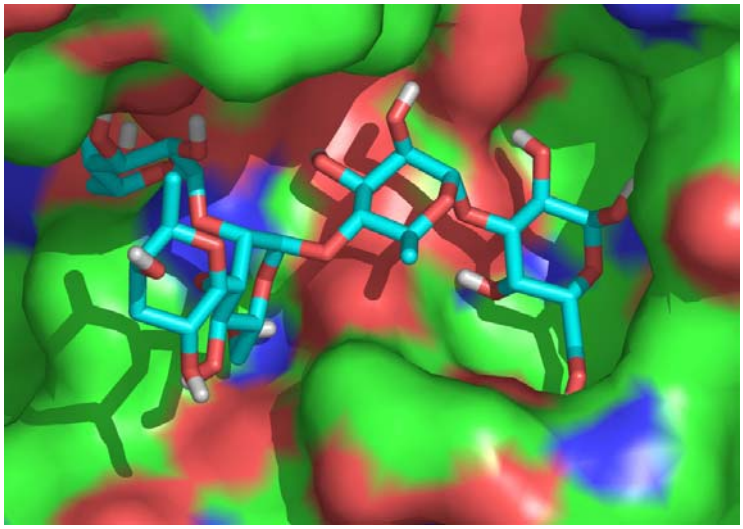

Figure 8. Surface representation with the best–docked pentasaccharide **4** (rhamnose in $^{1}C_{4}$, see Figures 6 and 7).

The best–docked conformation of the second major cluster with pentasaccharide **4** (13/50 conformations; $\Delta G_{binding}$: –8.21 kcal/mol) is shown in Figure 9. Surprisingly, the C5–methylgroup of the L–rhamnose in subsite –1 is now pointing towards Trp391, as seen in the dockings with tetrasaccharides **1** and **2**, and as observed in the crystal structure. In this case, Glu359 is at a correct position and distance (4.6 Å) from C1 of the scissile glycosidic bond to serve as general base for activating a water–nucleophile. However, the oxygen of the scissile bond is now oriented in such a

way that none of its lone pairs are accessible for protonation by either Asp392 or Asp395.

Figure 9. Best–docked conformation of the higher energy 13/50 cluster with pentasaccharide **4** (rhamnose in $^1C_4$).

Missing a proton donor, this conformation must be discarded as a productive binding mode candidate. In a confirming experiment, the trisaccharide α–D–Man*p*–(1→4)–α–L–Rha*p*–(1→3)–α–D–Gal*p* (with the L–rhamnose in the $^1C_4$ chair) was also docked in the same grid box; it yielded a large 42/50 cluster of alike conformations with carbohydrate ring positionings in subsites –2 to +1 analogous to Figures 6–8, but not a single conformation as seen in Figure 9.

For completeness, the pentasaccharide **5** was docked as well, since this α–L–rhamnose $^1S_3$ ring conformation also has a ring–oxygen lone–pair that is antiperiplanar to the scissile bond (ALPH–compliant). This experiment however yielded a series of non–realistic binding modes, with carbohydrate ring positions that are seriously deviating from those in the previous clusters.

4 CONCLUSIONS

The presently described docking experiments strongly suggests that an ALPH–compliant inverting mechanism is operative on hydrolysis of the O–antigen substrate by the Family GH–90 *Salmonella* phage P22 tailspike protein, with an anti–positioned Asp395 acting as proton donor and with Asp392 as general base assistant.

Acknowledgment

T. D. acknowledges financial support by I. W. T. (Belgium). The authors wish to thank Dr. S. N. Savvides (Laboratory for Protein Biochemistry and Protein Engineering, Ghent University, Belgium) for carefully reading the manuscript and for fruitful discussions on interpreting crystallographic data.

5 REFERENCES

[1] J. V. Israel, T. F. Anderson and M. Levine, *In vitro* Morphogenesis of Phage P22 from Heads and Base–Plate Parts, *Proc. Natl. Acad. Sci. USA* **1967**, *57*, 284–291.

[2] J. V. Israel, A Model for the Adsorption of Phage P22 to *Salmonellum typhimuruim*, *J. Gen. Virol.* **1978**, *40*, 669–673.

[3] S. Iwashita and S. Kanegasaki, Enzymatic and Molecular Properties of Base–Plate Parts of Bacteriophage P22, *Eur. J. Biochem.* **1976**, *65*, 87–94.

[4] U. Eriksson and A. A. Lindberg, Adsorption of Phage P22 to *Salmonella typhimurium*, *J. Gen. Virol.* **1977**, *34*, 207–221.

[5] U. Eriksson, S. B. Svensson, J. Lönngren and A. A. Lindberg, *Salmonella* Phage Glycanases: Substrate Specificity of the Phage P22 *Endo*–rhamnosidase, *J. Gen. Virol.* **1979**, *43*, 503–511.

[6] E. T. Palva and H. Mäkelä, Lipopolysaccharide Heterogeneity in *Salmonella typhimurium* Analyzed by Sodium Dodecyl Sulphate/Polyacrylamide Gel Electrophoresis, *Eur. J. Biochem.* **1980**, *107*, 137–143.

[7] B. –L. Chen and J. King, Thermal Unfolding Pathway for the Thermostable P22 Tailspike Endorhamnosidase, *Biochemistry* **1991**, *30*, 6260–6269.

[8] M. Danner, A. Fuchs, S. Miller and R. Seckler, Folding and Assembly of Phage P22 Tailspike Endorhamnosidase Lacking the N–Terminal, Head–Binding Domain, *Eur. J. Biochem.* **1993**, *215*, 653–661.

[9] U. Baxa, S. Steinbacher, S. Miller, A. Weintraub, R. Huber and R. Seckler, Interactions of Phage P22 Tails with Their Cellular Receptor, *Salmonella* O–Antigen Polysaccharide, *Biophys. J.* **1996**, *71*, 2040–2048.

[10] P. M. Coutinho and B. Henrissat, Carbohydrate–Active Enzymes: an Integrated Approach; in: *Recent Advances in Carbohydrate Engineering*, Eds. H. J. Gilbert, G. Davies, B. Henrissat and B. Svensson, The Royal Society of Chemistry, Cambridge, 1999, pp 3–12. URL: http://afmb.cnrs–mrs.fr/CAZY/.

[11] S. Steinbacher, R. Seckler, S. Miller, B. Steipe, R. Huber and P. Reinemer, Crystal Structure of P22 Tailspike Protein: Interdigitated Subunits in a Thermostable Trimer, *Science* **1994**, *265*, 383–386.

[12] S. Steinbacher, U. Baxa, S. Miller, A. Weintraub, R. Seckler and R. Huber, Crystal Structure of Phage P22 Tailspike Protein Complexed with *Salmonella sp*. O–Antigen Receptors, *Proc. Natl. Acad. Sci. USA* **1996**, *93*, 10584–10592.

[13] S. Steinbacher, S. Miller, U. Baxa, N. Budisa, A. Weintraub, R. Seckler and R. Huber, Phage P22 Tailspike Protein: Crystal Structure of the Head–Binding Domain at 2.3 Å, Fully Refined Structure of the Endorhamnosidase at 1.56 Å Resolution, and the Molecular Basis of O–Antigen Recognition and Cleavage, *J. Mol. Biol.* **1997**, *267*, 865–880.

[14] C. L. Perrin, R. E. Engler and D. B. Young, Bifunctional Catalysis and Apparent Stereoelectronic Control in Hydrolysis of Cyclic Imidatonium Ions, *J. Am. Chem. Soc.* **2000**, *122*, 4877–4881.

[15] A. J. Kirby, *The Anomeric Effect and Related Stereoelectronic Effects at Oxygen*, Springer–Verlag, Berlin, 1983.

[16] P. Deslongchamps, *Stereoelectronic Effects in Organic Chemistry*, Pergamon Press, Oxford, 1983.

[17] E. Lorthiois, M. Meyyappan and A. Vasella, β–Glycosidase Inhibitors Mimicking the Pyranoside Boat Conformation, *Chem. Commun.* **2000**, 1829–1830.

[18] P. Deslongchamps, Intramolecular Strategies and Stereoelectronic Effects – Glycosides Hydrolysis Revisited, *Pure & Appl. Chem.* **1993**, *65*, 1161–1178.

[19] A. Vasella, G. J. Davies and M. Böhm, Glycosidase Mechanisms, *Curr. Opin. Chem. Biol.* **2002**, *6*, 619–629.

[20] G. M. Morris, D. S. Goodsell, R. S. Halliday, R. Huey, W. E. Hart, R. K. Belew and A. J. Olson, Automated Docking Using a Lamarckian Genetic Algorithm and an Empirical Binding Free Energy Function, *J. Comput. Chem.* **1998**, *19*, 1639–1662.

[21] W. E. Hart, T. E. Kammeyer and R. K. Belew, The Role of Development in Genetic Algorithms, in: *Foundations of Genetic Algorithms III*, Eds. D. Whitley and M. Vose, Morgan Kauffman, San Francisco, CA. 1994, pp 315–

332.

[22] R. K. Belew and M. Mitchell, *Adaptive Individuals in Evolving Populations: Models and Algorithms*, Santa Fe Institute Studies in the Science of Complexity, XXVI, Addison–Wesley, Reading, MA., 1996.

[23] M. F. Sanner, Python: a Programming Language for Software Integration and Development, *J. Mol. Graphics Mod*. **1999**, 17, 57–61.

[24] N. Guex and M. C. Peitsch, Swiss–Model and the Swiss–PDB Viewer: an Environment for Comparative Protein Modeling, *Electrophoresis* **1997**, *18*, 2714–2723. URL: http://www.expasy.org/spdbv/.

[25] N. L. Allinger, MM2. A Hydrocarbon Force Field Utilizing v_1 and v_2 Torsional Terms, *J. Am. Chem. Soc*. **1997**, 99, 8127–8134.

[26] U. Burkert and N. L. Allinger, *Molecular Mechanics*, ACS Monograph 177, American Chemical Society, Washington, DC, 1982.

[27] J. Gasteiger and M. Marsili, Iterative Partial Equalization of Orbital Electronegativity – a Rapid Access to Atomic Charges, *Tetrahedron* **1980**, *36*, 3219–3228.

[28] W. D. Cornell, P. Cieplak, C. I. Bayly, I. R. Gould, K. M. Merz Jr., D. M. Ferguson, D. C. Spellmeyer, T. Fox, J. W. Caldwell and P. A. Kollman, A Second Generation Force–Field for the Simulation of Proteins, Nucleic Acids, and Organic Molecules, *J. Am. Chem. Soc*. **1995**, *117*, 5179–5197.

[29] P. F. W. Stouten, C. Frömmel, H. Nakamura and C. Sander, An Effective Solvation Term Based on Atomic Occupancies for Use in Protein Simulations, *Molecular Simulations* **1993**, *10*, 97–120.

[30] F. J. Solis and R. J.–B. Wets, Minimization by Random Search Techniques, *Math. Oper. Res*. **1981**, *6*, 19–30.

[31] W. E. Hart, *Adaptive Global Optimization with Local Search*, Ph.D. Thesis, Computer Science and Engineering Department, University of California, San Diego, 1994. See ftp://ftp.cs.sandia.gov/pub/papers/wehart/pre1996/thesis.ps.gz.

[32] W. L. DeLano, *The PyMOL Molecular Graphics System*, DeLano Scientific, San Carlos, CA., 2002. URL: http://www.pymol.org.

[33] T. D. Heightman and A. T. Vasella, Recent Insights into Inhibition, Structure, and Mechanism of Configuration–Retaining Glycosidases, *Angew. Chem. Int. Ed. Engl*. **1999**, *38*, 751–770.